

# Curvature- and Model-Based Surface Hatching of Anatomical Structures Derived from Clinical Volume Datasets

Rocco Gasteiger, Christian Tietjen, Alexandra Baer, and Bernhard Preim

Otto-von-Guericke University of Magdeburg,  
Department of Simulation and Graphics, Germany  
gasteiger@isg.cs.uni-magdeburg.de

**Abstract.** We present a texture-based method to hatch anatomical structures derived from clinical volume datasets. We consider intervention planning, where object and shape recognition are supported by adding hatching lines to the anatomical model. The major contribution of this paper is to enhance the curvature-based hatching of anatomical surfaces by incorporating model-based preferential directions of the underlying anatomical structures. For this purpose, we apply our method on vessels and elongated muscles. Additionally, the whole hatching process is performed without time-consuming user interaction for defining stroke direction and surface parameterization. Moreover, our approach fulfills requirements for interactive explorations like frame coherence and real time capability.

## 1 Introduction

For intervention planning, e.g., surgery or interventional radiology, medical doctors need a precise mental understanding of the anatomy of the particular patient. The planning is performed on individual patient datasets with reduced resolution and noise artifacts, which impedes the analysis more complicate. For this purpose, hatching offers a great potential because it is traditionally used for shading in anatomical illustrations, facilitating structure distinctions, and describing local shape characteristics. The latter one was investigated by Kim et al. [1] who have shown that lines along curvature directions improve the human shape perception compared to a simple shading or arbitrary directions. Applied to semi-transparent surfaces, these lines expose internal objects where important shape characteristics like concave and convex regions are still noticeable. Due to the characteristics of anatomical models and the quality of datasets, common hatching approaches which are only based on curvature information, are not appropriate.

In this paper we focus on hatching of anatomical surfaces within intervention planning. We consider vessels and elongated muscles and derive model-based preferential directions. These directions are combined with curvature information to determine the final hatching direction. Since intervention planning is a routine

task, we aim at a non-manual specification of hatching directions and no time-consuming parameter settings. Furthermore, we require frame coherence and real time capability for interactive exploration. Based on the resulting direction field, we perform a texture-based approach to apply line textures to the anatomical structures. This leads to a new contribution of shape enhancement within the intervention planning.

## 2 Related Work

Existing hatching techniques can be classified as image-, object- and texture-based approaches. Hertzmann and Zorin [2] compute principle curvature directions and introduce an optimization method to create geodesic streamlines by projecting them into the image space. Additionally, the authors point out that many parameter settings are necessary for their rendering result. Rössl and Kobbelt [3] additionally apply user-defined reference directions in the image plane to align the curvature directions. Ritter et al. [4] generate hatching strokes for smoothed vessel surfaces by calculating differences of several depth buffer images. Although they produce convincing results, frame coherence is not ensured by these methods. For object-based methods hatching lines are completely generated onto the 3D surface of an object. Most of the object-based approaches also compute principle curvature information for each vertex and align polygonal lines to them [5], [6], [7]. Zander et al. [7] use an extension of the optimization method from [2] to smooth the vector field. Since the lines are attached to the surface, frame-coherent renderings are achieved. However, hatching lines are only aligned to curvature directions. In addition, [6] have limited real time capabilities and [7] involves complex parameter settings to depict contrast images. Deussen et al. [8] introduce non-curvature alignment by generating lines by intersecting the geometry with a set of individually placed planes. The computation of a geometric skeleton allows to automatically determine the orientation of the intersection planes. However, the skeleton algorithm is not particularly appropriate for complex or branching objects like vessel structures. The main challenge for texture-based approaches is to determine appropriate texture coordinates for mapping 2D images onto a complex 3D surface with low distortions. Praun et al. [9] introduce *lapped patches* to combine local parameterization with local alignment to an underlying vector field. They use texture blending to reduce texture seams at patch boundaries and to perform real time capability and frame coherence. They extend their approach with *Tonal Art Maps* (TAM) for a light and view depending hatching with spatial and temporal coherence [10].

## 3 Requirement Analysis

Hatching of common anatomical structures for intervention planning is a challenging task. Several approaches may generate pleasant results, but lack one or more of requirements for use in intervention planning. Most methods align

hatching strokes only along curvature information or require some user interaction to place reference lines. However, curvature information do not describe model-based directions, such fiber directions of a muscle. Furthermore, model-based directions cannot be extracted directly from images of common clinical CT or MRI data. Instead, a surface description has to be derived. For anatomical structures common representation are polygonal representations. In addition to curvature information, model-based directions have to be extracted automatically from these surfaces. The surfaces are extracted from binary segmentation masks, which need to be smoothed to eliminate the staircase artifacts. The remaining artifacts lead to a complex surface with respect to the number of convex and concave vertices. Therefore, correct curvature estimations suffer from these artifacts.

We employ a texture-based technique since it is as fast as image-based techniques and frame-coherent like object-based approaches. The quality of the texture mapping strongly depends on the underlying surface parameterization. Since we are interested in the local alignment of hatching strokes, we choose *lapped patches* [9] as an appropriate surface parameterization.

## 4 Curvature- and Model-Based Vector Field

In the following we describe an approach to automatically generate a curvature- and model-based vector field for vessel structures and elongated muscles. Based on our observations from anatomic textbooks, vessels and muscles have a global specific preferential direction. The hatching lines run radially around vessel surfaces and along the fiber direction for muscle structures. For organs, there exists no such model-based direction. The illustrator chooses the line orientation that depicts the surface shape most suitable from the current viewpoint. Hence, we do not consider this type of anatomical structure in the paper. It is noticeable that curvature information are not sufficient to generate all aforementioned model-based directions. Although the radial alignment for vessel structures theoretically corresponds to the first principle curvature direction, this does not hold for rough vessel surfaces derived from routine medical image data. The corresponding directions contain noise that has no radial orientation. Furthermore, fiber directions cannot be described by curvature, which also introduces singularities (see Fig. 1(a)).

In the following, we perform three steps to automatically get a shape enhanced, frame-coherent and almost non-singular model-based vector field depending on the underlying anatomical surface:

1. Adaptive curvature estimation (Fig. 1(a)),
2. Definition of a model-based preferential direction (Fig. 1(b)), and
3. Combination of 1 and 2 to the final vector field (Fig. 1(c)).

The latter one resolves singularities for vessels and muscles because of their inherent preferential direction. For automatic determination for which anatomical structure its preferential direction has to compute, the structure type (vessel,

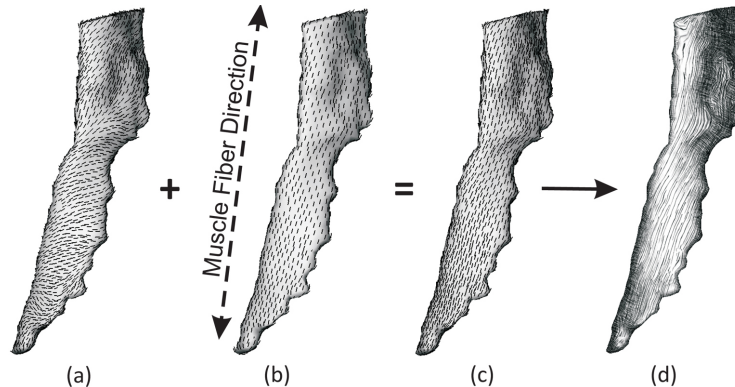


**Fig. 1.** Pipeline of our hatching approach: (a) curvature estimation, (b) approximation of preferential direction (depicted as arrow), and (c) combination of (a) and (b) to the final model-based vector field, (d) employing TAM textures aligned to the vector field.

muscle) is stored to the dataset during the prior segmentation process. Finally, we apply hatch textures (e.g., TAM’s) onto the surface with lapped patches (Fig. 1(d)). For a more precise description of each processing step, we refer to our technical report [11]. Additionally, more results are presented therein.

#### 4.1 Adaptive Curvature Approximation

At first we apply a Laplace filter to smooth a copy of the anatomical surface. On this instance, we estimate the curvature direction used for each original vertex  $p$ . Due to the simple surface topology (number of convex and concave vertices) of muscle structures, we select a quadratic surface fitting method with topology-independent parameterization according to [12]. Vessel structures exhibit a more complex surface where a topology-independent parameterization does not always preserve the ordering of neighbors around  $p$ . Hence, we select a topology-dependent parameterization by approximation of geodesic polar coordinates of each  $p$  according to Rössl et al. [5].

#### 4.2 Model-Based Preferential Directions

In order to obtain model-based preferential directions, we employ the internal skeleton of each structure to derive their preferential directions (inspired by Deussen et al. [8] and Roessl et al. [3]). For **vessel structures**, we extract the internal skeleton by the skeletonization algorithm presented in [13]. Based on the segmented voxel dataset this method combines topological thinning with distance transformation. With an appropriate sensitivity parameter, irrelevant side branches are effectively removed. The result of the skeletonization is a graph  $G$  which contains the edges  $e_i$  as connections between different branchings. Each edge consists of individual skeleton voxels  $s_j$ .

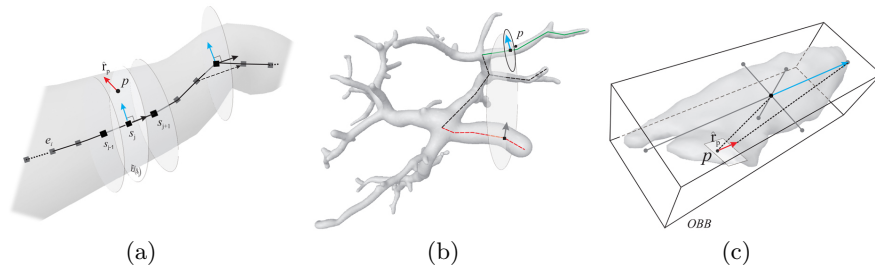


**Fig. 2.** Definition of the preferential direction  $\hat{r}_p$  at a vertex  $p$  by internal skeletons for (a, b) vessel and (c) muscle structures: (a) Projection of the "up" vector (blue) of the corresponding intersection plane  $E(s_j)$  (b) into the tangent plane of  $p$  as  $\hat{r}_p$  (red), (c) Approximation of the skeleton by the *OBB* and choosing the longest axis (blue) as  $\hat{r}_p$ .

The local radial alignment for vessel structures corresponds to the direction which is perpendicular to the local direction of the skeleton course. To compute such a vector, we need the nearest local skeleton direction for each vertex. Fig. 2(a) illustrates a vessel section with its corresponding edge  $e_i$  and some skeleton voxels as black squares. Through each  $s_j$  we place a plane  $E(s_j)$  (circular disk) defined by  $s_j$  and its direction vector (black arrow). The latter one is calculated by central differences of its two incident skeleton voxels  $\|s_{j+1} - s_{j-1}\|$ . Additionally, we determine the nearest plane  $E(s_j)$  to  $p$ . The "up"-vector (blue arrow) that is perpendicular to the direction vector, lies within  $E(s_j)$  and describes the local radial direction of  $p$ . The projected vector of this direction to the tangent plane of  $p$  is the local (normalized) preferential vector  $\hat{r}_p$  for  $p$ . For complex vessels we firstly determine the corresponding skeleton edge  $e_i$  for each vertex  $p$  before the nearest plane is selected. This requirement is illustrated in Fig. 2(b) where the vascular tree of the liver is shown. There are two planes nearby at  $p$ , but only the green line with the bordered plane, is the corresponding edge to  $p$  to get the right local "up"-vector.

For **elongated muscle structures**, we have to define the fiber direction which indicates the course between origin and onset of the muscle. We simply approximate this orientation by the longest principle axis of the object-oriented bounding box (*OBB*). Fig. 2(c) shows a muscle structure surrounded by its *OBB* as well as the corresponding principle axes. Among all three directions the vector  $\mathbf{u}$  is the longest one and we define  $\hat{r}_p$  as the projection of  $\mathbf{u}$  to the tangent plane of each  $p$ .

### 4.3 Combination of Curvature and Preferential Direction

With the aforementioned approach, we obtain two kinds of direction information for vessel and muscle structures at each vertex  $p$ : curvature information in terms of both principle directions, and preferential direction  $\hat{r}_p$  depending on the underlying anatomical structure. In the following, we combine this information to a stable vector field, which takes local curvature behavior into account. In Fig. 3(a)

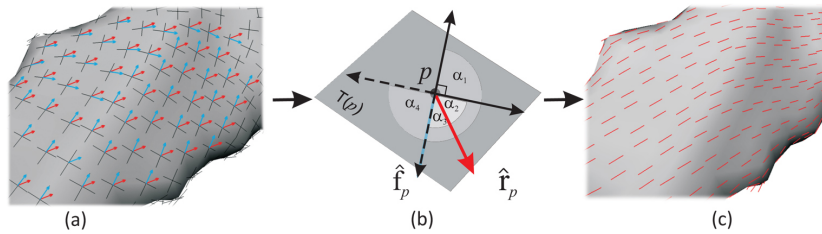


**Fig. 3.** (a) Curvature information (crosses) and preferential direction (red arrow= $\hat{r}_p$ ) at each vertex  $p$ , (b) Selection of the principle direction which has the smallest angle to  $\hat{r}_p$  and denote it as  $\hat{f}_p$ , (c) Resulting and optimized model-based vector field.

for each vertex its two principle directions are shown as black crosses and one preferential direction is shown as red arrow. Fig. 3(b) illustrates all directions for one vertex  $p$  within its tangent plane  $T(p)$ . Additionally, the enclosed angles between  $\hat{r}_p$  and all four possible principle directions are included. For the initial vector field, we select the principle direction which has the smallest angle  $\alpha_i$  ( $i \in 1, 2, 3, 4$ ) to  $\hat{r}_p$  and denote this direction as  $\hat{f}_p$ , indicated by a blue arrow.

The resulting vector field has still discontinuities (Fig. 3(a)), where each selected principle direction is highlighted (blue). We improve the alignment of each  $\hat{f}_p$  to the preferential direction  $\hat{r}_p$  and to its neighborhood. This means we aspire to a global geodesic course of the vector field. We use an energy minimization problem. For each optimization step, we rotate  $\hat{f}_p$  into the direction of  $\hat{r}_p$  and calculate the average angular deviation to all  $\hat{f}_i$ . The rotation stops, if the angle between  $\hat{f}_p$  and  $\hat{r}_p$  as well as the angular deviation becomes larger in comparison to the previous step. For each vertex we perform this operation recursively until the optimization is minimized. Finally, we compute a direction vector for every face by averaging the directions of the face vertices. Since we prefer a line adjustment that is more aligned to the preferential direction, the aforementioned simplified optimization method is sufficient. Fig. 1(c) and Fig. 3(c) show results after the optimization. A geodesic vector field is computed without singularities, aligned to the preferential direction, and includes local curvature behavior.

## 5 Results and Discussions

All presented results do not need any user interaction and were processed on a Pentium 4 processor with 3.2GHz and NVIDIA Quadro FX2000 GPU. Depending on mesh resolution each dataset needs some preprocessing time to calculate the vector field and surface parameterization, which is noticed for each example. During the rendering, we obtain real time capability and frame coherence. Computed texture coordinates are stored to each surface for further renderings.

Fig. 4(a) shows the resulting hatching on a neck vessel (preprocessing of 10 seconds with 878 faces) with a simple line texture. As shown in the rendering, the hatching lines have a radial orientation, and in spite of the rough surface no

strong texture distortions are visible. The TAM concept is employed in Fig. 4(c) for a neck muscle (preprocessing of 30 seconds with 2749 faces) to depict light conditions. It is noticeable that TAM texturing supports the depiction of convex and concave regions. However, for regions with low illumination the dark tones hide surface characteristics, noticeable at the shape boundaries of the muscle. Fig. 4(c) shows a scene of neck surgery planning. Surgical decisions for neck dissections are depending on the relative position between lymph nodes (yellow) and muscles (brown). Hence, lymph nodes as focus structures are opaque, bones (gray) and muscles are semi-transparent. Additionally, all structures are highlighted with their silhouettes. We applied a simple line texture with opacity mapping on the muscles, generated with our hatching approach. It needs a one-time preprocessing of 30 seconds for both muscles (5620 faces). Lymph nodes behind the muscles are still visible, but muscle surfaces obtain a more precise description. Additionally, the fiber direction is depicting and facilitates the structure distinction to surrounded objects.

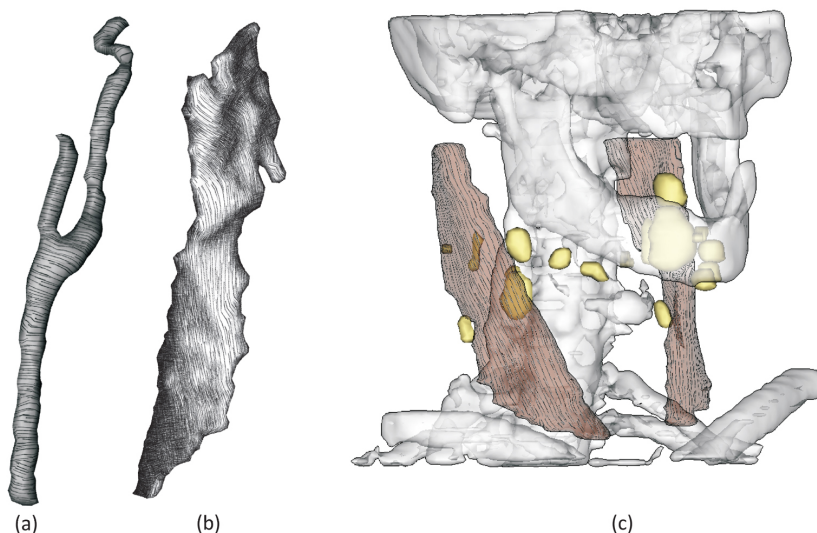


**Fig. 4.** (a) Hatching a neck vessel with a simple line texture, (b) Our approach applied with TAM textures to a neck muscle, (c) Opacity mapping of simple line textures to two neck muscles within a scene of neck surgery planning.

## 6 Conclusions and Future Work

We developed a model-based hatching approach for anatomical surfaces, in particular for vascular and elongated muscle structures derived from clinical volume datasets. Our novel combination of curvature and preferential direction information depicts local shape characteristics and supports structure distinctions.

Avoiding time-consuming user interaction, providing real time capability, and frame coherence makes our approach applicable for intervention planning or visualizations in anatomical education. Additional shape perception is supported in contrast to a simple color shading, especially for semi-transparent context structures. For future work we intend to determine preferential directions for more anatomic or complex structures, e.g., bones or other muscle types.

**Acknowledgment** We thank MeVis Research for providing advanced MeVisLab features.

## References

1. Kim, S., Hagh-Shenas, H., Interrante, V.: Showing Shape with Texture: Two Directions Seem Better than One. In: SPIE Human Vision and Electronic Imaging. (2003) 332–339
2. Hertzmann, A., Zorin, D.: Illustrating Smooth Surfaces. In: SIGGRAPH. (2000) 517–526
3. Rössl, C., Kobbelt, L.: Line-Art Rendering of 3D-Models. Pacific Graphics (2000) 87–96
4. Ritter, F., Hansen, C., Dicken, V., Konrad-Verse, O., Preim, B., Peitgen, H.O.: Real-Time Illustration of Vascular Structures for Surgery. IEEE Transactions on Visualization **12** (2006) 877–884
5. Rössl, C., Kobbelt, L., Seidel, H.P.: Line Art Rendering of Triangulated Surfaces using Discrete Lines of Curvature. In: WSCG. (2000) 168–175
6. Sousa, M.C., Samavati, F.F., Brunn, M.: Depicting Shape Features with Directional Strokes and Spotlighting. In: Computer Graphics International. (2004) 214–221
7. Zander, J., Isenberg, T., Schlechtweg, S., Strothotte, T.: High Quality Hatching. Computer Graphics Forum **23**(3) (2004) 421–430
8. Deussen, O., Hamel, J., Raab, A., Schlechtweg, S., Strothotte, T.: An Illustration Technique Using Hardware-Based Intersections. In: Proc. of Graphics Interface. (1999) 175–182
9. Praun, E., Finkelstein, A., Hoppe, H.: Lapped Textures. SIGGRAPH (2000) 465–470
10. Praun, E., Hoppe, H., Webb, M., Finkelstein, A.: Real-Time Hatching. In: SIGGRAPH. (2001) 581–586
11. Gasteiger, R., Tietjen, C., Baer, A., Preim, B.: Curvature- and model-based surface hatching of anatomical structures derived from medical volume datasets. Technical report, University of Magdeburg, Department of Simulation and Graphics (2008)
12. Goldfeather, J.: Understanding Errors in Approximating Principal Direction Vectors. Technical report, University of Minnesota, Department of Computer Science and Engineering (2003)
13. Selle, D., Spindler, W., Preim, B., Peitgen, H.O. In: Mathematical Methods in Medical Image Processing: Analysis of Vascular Structures for Preoperative Planning in Liver Surgery. Springer (2000) 1039–1059